

Enhanced and rapid photocatalytic degradation of toxic dyes by Cobalt oxide and modified Cobalt oxide under solar light irradiation

Debapriya Pradhan¹, Ermelinda Falletta^{2,3}, Suresh Kumar Dash^{1*}

¹ Department of Chemistry, ITER, Siksha 'O' Anusandhan (Deemed to be University), Bhubaneswar, Odisha 751030, India

² Department of Chemistry, Università degli Studi di Milano, via C. Golgi 19, 20133, Milano, Italy

³ Consorzio Interuniversitario Nazionale per la Scienza e Tecnologia dei Materiali (INSTM), via Giusti 9, 50121 Florence, Italy

*Corresponding author. Email address; sureshdash@soa.ac.in

Abstract

A solar light driven photodegradation approach for methylene blue (MB, model molecule of the thiazine dyes class) and malachite green (MG, model molecule of the triphenylmethane category) abatement by Co_3O_4 and $\text{Cr-Co}_3\text{O}_4$ spinel nanoparticles is reported. The effect of chromium load (5, 10 and 15%) in Co_3O_4 particles, synthesized by a simple co-precipitation process, was properly studied. The structural and morphological characteristics, chemical composition and optical properties of the materials were investigated by X-ray diffraction (XRD), Transmission Electron Microscopy (TEM), Field Emission Scanning Electron Microscopy – Energy Dispersive Spectroscopy (FE-SEM-EDS), FT-IR spectroscopy, UV-Vis diffuse reflectance spectroscopy (DRS), photoluminescence (PL) and BET surface area analysis. It was observed that properly tuning the initial pH, the initial dye concentration, the agitation time, and the photocatalyst dose, (10)Cr- Co_3O_4 exhibited an enhanced photocatalytic activity compared to that of pristine Co_3O_4 , demonstrating the positive role of Cr doping. In fact, the PL investigation showed that Cr doping in the Co_3O_4 lattice greatly increase the separation of electron-hole (e^-/h^+) pairs, whereas the UV DRS spectra and Tauc plot revealed a decrease in the band gap energy for Cr- Co_3O_4 . The investigations demonstrated that the MB dye degradation increases from 88% to 96% at pH = 11 after doping of Co_3O_4 by 10% of Cr. Similarly, the Cr doping allowed to enhance the MG dye degradation from 85% to 92% at pH = 9. The photodegradation kinetics of both MB and MG dyes by Cr- Co_3O_4 and Co_3O_4 NPs were of pseudo-first-order mode. The active species involved in the photocatalytic process were properly identified using various scavengers by trapping holes and radicals. Finally, the photocatalysts showed good stability during recycling maintaining high performances after 5-time usage.

Keywords: Co_3O_4 , Cr- Co_3O_4 , toxic dyes, photodegradation, solar light.

Introduction

The continuously increasing water pollution represents a global concern for the daily life. It is mainly related to the environmental degradation due to rapid urbanisation, massive industrialisation and improper waste management [1]. More in detail, industrial effluents containing organic dyes as contaminants are extremely harmful to human physiology causing vomiting, nausea, and endocrine disruption even at meagre concentrations leading to threat to good health [2]. Textile, leather tanning and finishing industrial effluents generally contain 10–15% of organic dyes that make the waste containing them carcinogenic and mutagenic [3]. The recalcitrant and complex structure of organic dyes makes hard any their degradation and/or mineralization [4]. A variety of physical, chemical, and biological techniques, such as adsorption, coagulation/flocculation, reverse osmosis, ultra filtration, electrochemical degradation, ozone oxidation, hybrid biological treatment, have been reported for the removal of toxic dyes from surface water [5-8]. However, photocatalysts typically have some practical limits such as a smaller specific surface area, lower adsorption performance, and a higher recombination rate of photogenerated electron-hole-pairs, which primarily limit industrial photo catalysis applications in organic wastewater treatment [9]. In the last years, the development of more sustainable approaches based on the potential use of a green and renewable source of light, such as solar irradiation, for the photocatalytic degradation of dyes by using semiconductors, perovskites and spinels, as photocatalysts has sparked considerable interest. Graphitic carbon nitride-based photocatalysts were used for efficient organic transformation as well as photocatalytic conversion of carbon dioxide to value-added compounds and renewable fuels [10-11]. The most appealing characteristics that attract researchers to focus on heterogeneous photocatalysts are the use of ambient conditions to carry out the reactions, the reusability, non-toxicity and low cost of the materials, and the possibility for various catalysts to be supported [12]. Over the last few decades, we have seen extensive and extraordinary research in the field of advanced oxidation processes (AOPs), which are regarded as the most promising method for the removal of pollutants, including organic, inorganic, and microbial contaminants, when compared to traditional purification procedures. AOPs produce highly reactive oxygen species (ROS) with high oxidising ability, such as $\cdot\text{OH}$, $\cdot\text{O}_2^-$, h^+ , and $\text{HO}_2\cdot$. These species can oxidise organic contaminants to CO_2 and inorganic ions, reduce inorganic contaminants to nontoxic ions, and inactivate microorganisms that produce no noxious compounds [13]. In this context, Yong Liu *et al.* demonstrated that g- C_3N_4 doped with 2 wt% NiFe_2O_4 led to a fast degradation of methylene orange dye when exposed to visible light. Similarly, 50 wt% g- C_3N_4 doped CoFe_2O_4 showed 94% degradation under visible light. Moreover, $\text{NiCr}_2\text{O}_4\text{-Bi}_2\text{O}_3$ and $\text{FeV}_2\text{O}_4\text{-Bi}_2\text{O}_3$ composites gave 93.4%, 91.4% of degradation efficiency towards MB dye in 120 and 160 min, respectively under UV light irradiation [14-18]. Shojaei and co-workers investigated the photocatalytic activity of $\text{CoCr}_2\text{O}_4/\text{TiO}_2$ composites showing a degradation efficiency of 90% towards MB dye in 90 min under visible light [19]. Ghiyasiyan-Arani compared pure FeVO_4 with a sono-chemically synthesised $\text{FeVO}_4/\text{V}_2\text{O}_5$ nano-composite that showed greater degradation efficiency towards Rhodamine B dye [20].

Recently, among spinels-based materials, cobalt oxide Co_3O_4 , has been quickly identified among the most interesting spinels, due to its thermal and chemical stability, and simple production process.[21]. Co_3O_4 follows the conventional spinel crystal structure AB_2O_4 ($\text{A} = \text{Co}^{2+}$, $\text{B} = \text{Co}^{3+}$), where Co^{2+} ions occupy 1/8th of tetrahedral A sites

and Co^{3+} ions occupy 1/2nd of octahedral B site. . This distinctive structure permits an easy movement of electrons between Co^{2+} and Co^{3+} ions, improving its photocatalytic activity also under visible light irradiation [22]. Conventional synthetic methods for Co_3O_4 , such as hydrothermal treatment, polymer combustion, microwave assisted and thermal decomposition were adopted that were cumbersome [23-26]. However, sol-gel synthesis and co-condensation processes were highly acclaimed for their simplicity and ease of operation as the prepared cobalt oxides had application in various fields such as lithium ion batteries, heterogeneous catalysts, gas sensors, ceramics, energy storage devices [27-29].

When used as photocatalysts, the major disadvantage of cobalt oxide it is related to its fast electron hole recombination which hampers in its photo degradation efficiency. Metals doping positively affects the crystallite particle size specific surface area, and the catalytic performance of these materials [30]. In particular, it was demonstrated that doping by Ni^{2+} , enhances the photocatalytic efficiency of the oxide towards the degradation of contaminants by inhibiting the electron-hole pairs recombination [31,32]. Along with Ni^{2+} , the effect of many other metal ions (Cu, Mn, etc.) have been properly investigated, demonstrating their ability to enhance the performance of cobalt oxide in the photocatalytic degradation of organic pollutants [33-35].

An important contribution also came from doping studies by transition metals ions. In this regard, Zr- Co_3O_4 was synthesized by a microwave-assisted technique, showing superior antibacterial activity, good optical transmission property in UV-DRS spectra and a band gap reduction with an increase in the amount of zirconium doping [36]. Sn-doped Co_3O_4 showed 75% of degradation efficiency against MB dye in 180 min under visible light [37], whereas Ag-doped Co_3O_4 exhibited high catalytic activity towards RhB dye degradation within a span of 30 min under visible light [38].

This work reports a simple sol-gel procedure for the synthesis of cobalt oxide nanoparticles (Co_3O_4) NPs and a co-precipitation method for the preparation of chromium doped cobalt oxide nanoparticles (Cr- Co_3O_4) NPs. The selection of chromium ions as doping agent, characterized by a large ionic radius, might be useful for creating lattice defects that could help for effective dye degradation. Its large ion radius ($R = 75.5\text{pm}$) generate an electron trapping defect site in pristine semiconductor helping to increase the surface sites [39]. Both oxides were used for the photocatalytic degradation of two toxic dyes MB (methylene blue) and MG (Malachite green) under solar light irradiation. The photodegradation kinetics of both MB and MG dyes were properly investigated, as well as the active species involved in the photocatalytic process. Finally, the stability of both the photocatalysts after 5-time usage was properly verified.

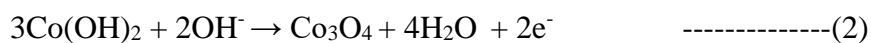
MATERIALS AND METHODS

2.1. MATERIALS

The synthesis of cobalt oxide was carried out by using cobalt nitrate hexahydrate (Merck, 99.9% purity) as a source. Chromium nitrate (Merck, 99.9% pure), ammonium hydroxide, and analytical-grade ethanol (Fisher Chem.) were used for the preparation of Cr-Co₃O₄. Malachite Green and Methylene Blue of analytical grade were purchased from Merck. Double distilled and deionized water was used for both syntheses and experimentation.

2.1.1. Synthesis of Co₃O₄

The Co₃O₄ NPs were prepared by sol-gel method previously reported [40]. 100 mL of 0.1M cobalt nitrate solution was introduced in a 250 mL beaker, and constantly stirred at room temperature for 30 minutes. Then, 100 mL of a 0.2 M sodium hydroxide solution was added drop wise under vigorously stirred. For the following 30 minutes, the solution was heated at 100°C. A pink gel was produced, which was centrifuged for 15 minutes at 5000 rpm before being filtered through a Buchner funnel. The resulting residue was dried at 100°C in an oven for three hours, and then calcined for three hours in a muffle furnace at 600°C[41]. The obtained powder was then ground into a fine powder by using a mortar and pestle for further experimental work. The chemical reactions occurred during Co₃O₄ synthesis are given below,



2.1.2. Synthesis of Cr-Co₃O₄

A co-precipitation method was adopted to synthesize chromium-doped Co₃O₄ particles having different percentages of chromium (5, 10, and 15 %). 100 mL of aqueous solution of 0.1 M Co(NO₃)₂.6H₂O and varying amounts of Cr(NO₃)₂ were prepared and subjected to stirring for 30 min. at room temperature. Then a solution of ammonia/ethanol (10 mL each) was added drop-wise to the previous solution and maintained under vigorous stirring for another 30 min. The synthesized gel was aged overnight in the same vessel. The day after, the obtained precipitate was filtered and washed with water for several times to remove the excess of ammonia and ethanol. The residual mass was dried in an oven at 100°C for 5hrs and then calcined at 600°C for 3hrs. [42]. The calcined material (Cr-Co₃O₄), was ground to a fine powder and used for further investigation. The obtained samples were labelled as (x) Cr-Co₃O₄ (where x=5, 10, and 15). The schematic diagram for synthesis of Cr-Co₃O₄ is given in Figure1.

2.2. Materials characterization

The crystallographic structure of the synthesized materials was investigated by X-ray diffraction (XRD) using a PAN analytical Diffractometer with Cu-K radiation (PW 1830,

Philips, Japan). A 2θ range of $10\text{-}80^\circ$ was used to acquire the diffraction patterns. Both a field emission scanning electron microscope (ZEISS SUPRA 55) and a high resolution transmission electron microscope (HR-TEM Jeol/JEM2100) were used to analyse the surface morphology of the synthesised oxides, while the chemical composition was investigated using EDS analysis. The synthesized compound was studied using FTIR spectrophotometer (Perkin Elmer Spectrum version 10.4.3) was used to determine the bond vibrational frequencies of the components, whereas a Perkin Elmer Lambda365 spectrophotometer was employed to acquire UV-DRS spectra (to investigate the materials' optical properties). Photoluminescence spectral (Dongwoo Optron DM 500i) analyses permitted the investigation of the photocatalysts optical and electrical characteristics. Lastly, for the analysis of the dyes' solutions before and after the photodegradation tests a UV-Vis spectrophotometer (Systronics 2202) was employed. A Brunauer Emmett Teller (BET) nitrogen adsorption/desorption instrument was used to determine the specific surface area and pore size (Quantachrome Instruments v11.05).

2.3. Photocatalytic tests

The photodegradation of MB and MG dyes was investigated using Co_3O_4 and $(\text{x})\text{Cr-Co}_3\text{O}_4$ NPs as the photocatalysts under solar light irradiation. To study the photocatalytic efficiency of the synthesized composite different parameters like pH, concentration, dose and time were taken into consideration. First of all, 0.1 g of each dye (MB and MG) was dissolved in 1L of distilled water to obtain two stock solutions of 100 ppm. Then, these solutions were appropriately diluted to 20, 40, 60, and 80 ppm. At the beginning, 20 mL of each solution was put in contact with an amount of 0.02 to 0.08 g of photocatalyst and stirred in the dark for 30 minutes to achieve adsorption-desorption equilibrium. Then, the mixture was kept under solar radiation under stirring for 120 minutes. During the reaction proper aliquots of solution were withdrawn, centrifuged to remove the photocatalyst, and filtered to examine the dye disappearance. The rate of decolourization was measured in terms of the intensity change of absorption peaks at 662nm and 614 nm for MB and MG, respectively [43-44].

2.4. Stability test

To demonstrate the stability and reusability of the photocatalysts, the synthesized oxides were reused for five runs. After each cycle the photocatalysts were filtered and washed by deionized water before being used again.

2.5. Active species trapping experiment

Benzoquinone (BQ), isopropyl alcohol (IPA), and disodium ethylenediaminetetraacetate (EDTA) were used as scavengers for holes (h^+), superoxide ($\text{O}_2^{\cdot-}$), and hydroxyl (OH^{\cdot}) radicals, respectively. The experimental methods were carried out as described in paragraph 2.3, but with an addition of 1 mmol of each scavenger.

2.6. TOC analysis

The level of mineralization of the dyes was determined by TOC analyses and evaluated by the following equation(3):

$$\% \text{ of dye mineralisation} = [(\text{TOC}_0 - \text{TOC}_t) / \text{TOC}_0] \times 100 \quad \text{-----}(3)$$

Where TOC_0 represents the initial organic carbon of the dye solution at '0' min and TOC_t represents the total organic carbon of the solution at time 't' min.

3. Results and Discussion

3.1 Materials Characterisation

An accurate and exhaustive characterization of Co_3O_4 and (10) Cr- Co_3O_4 is reported below.

Among the different doped materials, (10)Cr- Co_3O_4 was selected for its higher photocatalytic activities.

3.1.1 XRD Analysis

Figure2. shows the XRD patterns of the as-prepared Co_3O_4 and (x) Cr- Co_3O_4 nanoparticles. The high crystallinity of the samples was confirmed by the strong and sharp diffraction peaks.

More in detail, the obtained peaks at $2\theta = 31.31, 36.91, 38.60, 44.86, 59.40,$ and 65.30 , corresponding to (220), (311), (222), (400), (511), and (440) planes, closely match the cubic spinel Co_3O_4 phase with space group $\text{Fd}3\text{m}$ (JCPDS No. 80-1535) [45]. No more peaks for impurities were found. Even at higher doping percentages, chromium ions have been effectively embedded into cobalt lattice positions without altering crystal symmetry. The observed peak broadening with the increase of chromium percentage may be due to a lowered crystallite size which shown in Figure 2.B, that makes Cr- Co_3O_4 a superior photocatalyst compared to cobalt oxide NPs. By using the Debye-Scherrer equation (as given in equation 4) the particle size of both Co_3O_4 and Cr- Co_3O_4 was calculated and resulted to be 41.3 and 39.1 nm, respectively.

$$D = k \lambda / \beta \cos\theta \quad \text{-----} \quad (4)$$

Where D is the crystallite size, k is known as the Scherer's constant ($K=0.94$), λ is the X-ray wavelength (1.54178\AA), β is the full-width at half-maximum, θ is the Bragg's angle of the associated peak[46].

3.1.2 FTIR analysis

The FTIR spectrum of Co_3O_4 (Figure3. black line) displayed the band at 654 and 554 cm^{-1} that were ascribed to the stretching vibration of cobalt oxide. The band at 3420 cm^{-1} corresponds to the stretching and bending vibrations of hydroxyl (O-H) groups [47]. The presence of the Co-O bond in Co_3O_4 is confirmed by the band at 548.27 cm^{-1} related to the

tetrahedral coordination of Co^{+2} ions, whereas the second band at 656.3 cm^{-1} is attributed to the octahedral coordination of Co^{+3} ions [48].

The bands between 3200 and 3500 cm^{-1} and those at 1600 cm^{-1} are associated to the presence of water on the catalyst's surface. The hydroxyl groups of H_2O molecules present in the lattice cause the large absorption bands at 3446 and 1634 cm^{-1} , whereas C-O stretching vibrations provide tiny peaks at 562 and 660 cm^{-1} respectively. Peak positions for Cr doped cobalt oxide have shifted slightly. The peaks observed at 551.67 and 656.71 cm^{-1} demonstrated the preservation of the Co-O bond despite Cr doping [49].

3.1.3 FE-SEM and EDS analysis

FE-SEM and EDS permitted the morphological, and compositional investigation of Co_3O_4 and (10) Cr- Co_3O_4 NPs, as shown in Figure 4(A and B). The Co_3O_4 NPs showed a flake-shape morphology, whereas (10) Cr- Co_3O_4 particles were mainly composed of spheres of 40 nm of diameter (Figure 4A and Figure 4B). The different morphology of the two photocatalysts can be easily attributed to the different synthetic approach used for their preparation: co-precipitation method for Co_3O_4 , sol-gel reaction for (10) Cr- Co_3O_4 . Concerning the elemental composition of the two photocatalysts, EDS analyses demonstrated that for Co_3O_4 the Co:O atomic percentage ratio was a 3:4, according to the literature [46] and that the atomic percentage of Co, O and C was found to be 48.95, 39.12 and 12.43%, respectively (Figure 4C). For (10) Cr- Co_3O_4 , however, the percentage of C, Co, O, and Cr was 14.8, 47.2, 33.7, and 4.3 %, respectively (Figure 4D), whereas the Co:O ratio resulted to be 2.9:3.7.

3.1.4 High-resolution transmission electron spectroscopy (HRTEM)

The HR-TEM images of both Co_3O_4 and (10) Cr- Co_3O_4 , showed in Figure 5(A-D), display the uniformly dispersed cubical crystalline particles with some aggregated cluster. In Figure 5A, the crystal structure has homogenous cubes of pure cobalt oxide NPs [50]. The HR-TEM images of Cr- Co_3O_4 show a change in particle size and shape of the NPs caused by the substitution of Cr^{2+} with Co^{2+} ions. The polycrystalline morphology of the nanoparticles, which are evenly disseminated and have rough surfaces, is seen in the bright-field picture of the nanoparticles. To explore the size distribution of Cr- Co_3O_4 NPs, the particle size was also measured from the HRTEM picture, and a precise estimate in the diameter size of the nanoparticles was obtained (40 nm). The average particle sizes obtained from the TEM and the XRD crystallite sizes were in excellent agreement [51].

3.1.5 Photoluminescence analysis

The recombination, migration, and transfer of photo-generated electron-hole pairs may be investigated by PL spectra. Figure 6 displays the PL spectra of (10) Cr- Co_3O_4 and pure Co_3O_4 . Two distinct peaks at 325 and 660 nm were obtained for both (10) Cr- Co_3O_4 and Co_3O_4 . Pure Co_3O_4 displayed higher intensity, indicating a greater e^-/h^+ recombination [52]. In contrast, the decreased intensity of the peaks for (10) Cr- Co_3O_4 demonstrates that Cr doping played a vital role in preventing undesired charge pair recombination and, as a consequence, enhancing the photocatalytic activity [53].

3.1.6 UV-DRS spectra results

UV-Vis absorption spectroscopy was used to examine the optical absorption behaviour of the prepared photocatalysts; the findings are displayed in Figure 7. The band gap energy of (10) Cr-Co₃O₄ and pure Co₃O₄ were calculated from the Tauc plot by using equation (5),

$$(\epsilon h\nu)^2 = P (E_g - h\nu) \quad (5)$$

Where ϵ is the molar extinction coefficient, h is plank constant, ν is the frequency of light, E_g is the band gap energy and P is the arbitrary constant. As shown in Figure8. the photocatalysts showed a strong absorption edge in the plot and E_g was estimated by extrapolating the plot's linear section.

Two types of optical transitions were seen for Co₃O₄ and (10) Cr-Co₃O₄ having band gap energy of 1.5eV,2.6 eV and 1.5eV, 2.0 eV, respectively. The Cr doping tunes the Fermi energy levels in the lattice sites leading to a narrower band gap in (10) Cr-Co₃O₄ [54]. In (10)Cr-Co₃O₄ the lower band gap is due to O₂ → Co³⁺ (E_{g1}) charge transfer whereas for Co₃O₄ the higher band gap is associated with O₂ → Co²⁺ (E_{g2}) charge transfer [55].

3.1.7 BET Analysis

Brunauer-Emmett-Teller (BET) N₂ adsorption/desorption measurements were used to determine the textural properties of Co₃O₄ and (10)Cr-Co₃O₄ composite catalysts. Figure 9(A) depicts the N₂ adsorption/desorption isotherms of (10)Cr-Co₃O₄, which correspond to the typical type IV isotherm curve indicating a typical mesoporous material[57]. The surface area of (10)Cr-Co₃O₄ (48.67 m²/g) was significantly greater than that of Co₃O₄ (8.65 m²/g), probably due to defects formed in the doped catalyst during the synthesis process. The increased surface area of (10)Cr-Co₃O₄ (Figure 9B) supported the superior photocatalytic activity compared to pristine Co₃O₄. According to the BJH pore size distribution (Figure 9C), (10)Cr-Co₃O₄ has a pore volume of 0.283 cc/g and pore diameter [Dv(d)] of 1.985 nm[56].

3.1.8 Effect of different parameters on the photocatalytic activity

The photodegradation of MB and MG by Co₃O₄ and (x) Cr-Co₃O₄ was investigated under solar light irradiation by an insolation of 4000Wh/m² during the months of April to May. he absorption capability of the photocatalysts were evaluated in the dark for 30 min. The initial concentration of 20 mg/L was taken for both MB and MG dyes and 0.02g of the (x)Cr-Co₃O₄ catalysts were used during the investigation The quantity of adsorbed MB and MG was also calculated by the absorption spectrum (t=0). . The percentage of dye removal was calculated as given in equation (6),

$$\text{Percentage degradation} = (C_0 - C) / C_0 \times 100 \quad (6)$$

where C_0 is the concentration of dye at initial time $t=0$ and C is the concentration of the dye at a time t during agitation under light source. As displayed in Figure10. after light irradiation the degradation efficiency of (10) Cr-Co₃O₄ was found be highest as compared to (5)Cr-Co₃O₄ and (15)Cr-Co₃O₄ hence was selected for further photodegradation experiments and its

performances were compared to those of pristine Co_3O_4 . The greater number of active sites in (x)Cr- Co_3O_4 due to stoichiometric advantages facilitated the dye molecules with a higher adsorption capacity [58].

The impact of various factors to the photocatalytic activity such as pH, initial dye concentration, agitation time, and photocatalyst dose, were then examined with Co_3O_4 and (10)Cr- Co_3O_4 photocatalysts.

3.1.8.1 Effect of pH

In the photocatalysis investigation the pH of the solution is important as the formation of hydroxyl radicals, photo oxidation by the positive holes in valence band, and photo reduction by the electron in the conducting band resulting $\text{OH}\cdot$ radical depend greatly on the pH [59]. The pH_{PZC} of Co_3O_4 and (10)Cr- Co_3O_4 were around 7.5 hence the surface of the catalysts are zero charge at pH equal to pH_{PZC} . Therefore, the surface of the catalysts is negatively charged in alkaline medium, and positively charged in acidic medium [60]. According to the literature, in basic medium the hydroxyl groups on the surface of Co_3O_4 are deprotonated developing a negative surface charge facilitating the adsorption of cationic dyes MB and MG [55]. As shown in Figure 11, the highest degradation towards MB was 96% by (10)Cr- Co_3O_4 and 86% by Co_3O_4 at pH value of 11. For MG, 92% degradation was attained by (10)Cr- Co_3O_4 , whereas Co_3O_4 degraded 85% at pH = 9. The activity of MG at pH > 9 may be attributed to the solution in contact with the basal oxygen surface of the tetrahedral sheet that contained excess hydroxyls. The adsorption rate of MG dye decreases with increase in pH (pH \geq 9), then becomes constant up to pH 13. Such decrease may be assigned to the presence of dimers $(\text{MG}^+)_2$ [36].

3.1.8.2 Effect of reaction time

Figure 12, illustrates the impact of the agitation time on the photocatalytic degradation of MB and MG dyes by Co_3O_4 and (10)Cr- Co_3O_4 NPs at the optimum pH values of degradation (pH = 11 for MB and pH = 9 for MG). The percentage of degradation for both the dyes increased with agitation time up to 90 min and after that remained almost same. The rapid degradation occurred in the first 60 min and increased marginally until it reached equilibrium after 90 min. With increasing time, the concentration of dye in the solution decreased thus reducing the percentage of degradation, secondly, after attaining equilibrium the degradation becomes stagnant. Figure 12 (A-D) shows that the photodegradation of MB was 88 and 95% for Co_3O_4 and (10)Cr- Co_3O_4 , respectively in 90 min, whereas MG was degraded in percentage of 83 and 94%. The reduced photoactivity of the materials after 90 min may be due to the deposition of by-products on the surface of the catalysts [61].

3.1.8.3 Effect of Photocatalyst Dose

In order to evaluate the effect of the photocatalyst dose on the photoactivity of the material, the reaction was carried out in the presence of different amounts of photocatalyst (10, 20, 30, 40 mg). As shown in Figure 13, the results indicated that maximum MB degradation of 80 and

94% was found for Co_3O_4 and (10)Cr- Co_3O_4 respectively with a photocatalyst dose of 20 mg. For MG dye the maximum degradation of 85 and 96% was achieved in similar conditions by the use of 20 mg of photocatalyst. The increase in catalyst amount increases the number of active sites on the photocatalyst surface and greater number of defects with more grain boundaries that helps the production of more OH^\cdot radicals facilitating the degradation of the dye [62, 63]. By further increasing the dose over 20 mg the percentage degradation is reduced the reason may be due to increase in active sites on catalyst there is rapid exchange of dye molecules [64].

3.1.8.4 Effect of Initial Dye Concentration

The dye concentration variation in the range 20-80 ppm is useful for determining the kinetics of the reaction. As given in Figure 14, an optimum degradation efficiency of 83 and 94% towards MB and 85 and 96% towards MG by Co_3O_4 and (10)Cr- Co_3O_4 , respectively was achieved at an initial concentration of 40 ppm for both the dyes. At higher initial dye concentration there is a competition of dyes to get adsorbed on the catalyst surface which might have decreased the favourability for percentage of degradation probably preventing the active sites for dyes adsorption. Secondly, due to over population of dyes the incident photons on the catalyst surface were inhibited reducing the amount of active radicals responsible for photodegradation [65].

Table 1 displays a comparison among the results obtained in the present work for photodegradation of MB and MG and those reported in the scientific literature by differently modified Co_3O_4 using different light sources.

The results show the superior activity of (10) Cr- Co_3O_4 towards the two dyes photodegradation, because it leads to the abatement of the 96% of MB and of the 94% of MG in only 90 minutes, whereas the other semiconductors need longer time sometimes with poor results.

3.1.8.5 Photocatalytic degradation kinetics study

The kinetic studies of the photocatalytic degradation of MB and MG dyes by Co_3O_4 and (10)Cr- Co_3O_4 followed a pseudo-first-order kinetics, as given in equation (7),

$$Kt = \ln C_0/C \quad (7)$$

where K stands pseudo-first-order rate constant, t represents the time, and C and C_0 the dye concentrations at time t and $t=0$. As shown in Figure 15, the relationship between $\ln(C_0/C)$ and the irradiation time is a linear with positive slope that satisfies the first order model [4].

3.1.8.6 Reusability of the photocatalyst

For a viable photocatalyst in practical applications high stability is required. In order to evaluate the reusability of (10) Cr- Co_3O_4 , the photocatalysts was tested for five cycles. At the end of each cycle, the photocatalyst was recovered by centrifugation, dried for 4 hours at 60°C and reused. From the first to the last cycle the percentage of degradation ineffectually

changed from 94 to 88% for MB and 96 to 90% for MG (Figure16). The retention of spinel structure of the catalyst was established by the XRD pattern after five runs. As shown in Figure17. the XRD peaks of the fresh and used (10)Cr-Co₃O₄ patterns indicated that the catalyst maintained its crystalline structure even after five cycles, confirming its reusability and maintaining its high activity .

3.1.8.7 Reactive species trapping experiments

The process of photocatalytic degradation involves a number of photogenerated species, such as h⁺, OH[•], and O₂^{-•}, as important agents to mineralise dyes. Scavengers such as disodium ethylenediaminetetraacetic acid (Na₂-EDTA), p-benzoquinone (BQ), and isopropyl alcohol (IPA) were used to trap h⁺, OH[•], and O₂^{-•} Species, respectively. Figure 18 showed that the presence of BQ (an O₂^{-•} scavenger) drastically reduced the degradation of MB (from 94 to 30%) and that of MG (from 96 to 27%). This result proved superoxide radicals played a vital role during the photodegradation process. Also the agent IPA, used for determining the involvement of OH[•] Radicals caused a reduction of the percentage of degradation of both MB and MG, indicating the importance of hydroxyl radicals in photodegradation. In contrast, by the addition of EDTA (h⁺ ion scavenger) a minimal effect on the photocatalytic degradation of MB and MG dyes was observed, indicating the less involvement of h⁺ ions during the photo degradation process.

3.1.8.8 TOC analysis

The mineralization of MB and MG was determined using total organic carbon (TOC) analysis. Figure 19 depicts the percentage of mineralization of MB and MG using (10) Cr-Co₃O₄ nano composite. For both the dyes the percentage of mineralization increased with irradiation time, reaching 92% and 90%, respectively, indicating a quite complete degradation

3.2 Mechanism of Photodegradation under solar light

The mechanism of the photodegradation process throws a light on the efficiency and potentiality of the catalyst. It is known that a number of characteristics, such as band gap energy, surface area, particle size, shape, charge carrier movement, crystalline structure, the catalyst stability and ability to absorb solar radiation influence, affect the photocatalyst efficiency [82]. The band gap energy of pristine Co₃O₄ and (10)Cr-Co₃O₄ were 2.6 and 2.1eV respectively that indicated high efficiency in the formation of electron/holes when the photocatalyst is exposed to visible light. Solar irradiation with similar energy or more than the band gap energy resulted in excitation of electron from the valence band to the conduction band with formation of holes in the valence band. To expedite the photo excitation, chromium in the Co₃O₄ lattice improvised the trapping of electrons and holes and subsequently minimised the recombination rate [83]. The produced holes in VB transform the OH[•] into a OH[•] free radical, the excited electrons in CB convert O₂ into O₂^{-•} free radical. The protonation of the produced superoxide (O₂^{-•}) results in the production of hydroperoxyl radical (HO₂) and finally H₂O₂, which further dissociates into highly reactive hydroxyl radicals (OH[•]) [84]. As a result, the organic dyes can be oxidised and converted into H₂O and CO₂.

The possible mechanism of MB degradation by (10) Cr-Co₃O₄ was graphically shown in Figure 20.

4. Conclusion

Co₃O₄ photocatalyst was synthesized by sol-gel method and (x) Cr-Co₃O₄ by a simple coprecipitation method. Both the samples were properly characterized to evaluate the structural, compositional, morphological, electrical, and optical properties. XRD, FESEM and HR-TEM confirmed the spinel phase structure with particle size ranging from 18 to 50nm. The incorporation of Cr into Co₃O₄ has significantly enhanced the surface area of Cr-Co₃O₄ by seven times that increased the photo-catalytic activity. The photocatalytic degradation revealed that (10)Cr-Co₃O₄ showed greater degradation efficiency than Co₃O₄ due to its lower band gap energy. Maximum degradation of 96 and 94% was achieved towards MB and MG, respectively by (10) Cr-Co₃O₄ at high pH values in 90 min. The enhanced photocurrent generation, improved charge separation, and broader absorption spectrum of (10)Cr-Co₃O₄ boosted the photocatalytic efficiency tremendously. The stability and reusability of the most performing photocatalyst, (10) Cr-Co₃O₄, was proved after five consecutive runs maintaining high dyes photodegradation. It was demonstrated that the photocatalytic degradation of MB and MG is mostly driven by OH[•] and O₂^{•-} radicals. Based on the above findings, the (10)Cr-Co₃O₄ NPs could be a potential alternative to existing photocatalysts for harmful dyes photodegradation that generally are present in industrial effluents.

Acknowledgments

The authors are grateful to the Department of chemistry, ITER, Siksha 'O' Anusandhan (Deemed To Be University), Bhubaneswar, for providing the help in experimentation and chemicals procured. We are thankful to the people of Material Analysis & Research Centre, Bengaluru, for carrying out the BET analysis within required time.

5. References

- [1] S. Borthakur, L. Saikia, ZnFe₂O₄@g-C₃N₄ Nanocomposites: An Efficient Catalyst for Fenton-like photo degradation of Environmentally Pollutant Rhodamine B, *J. Env. Chem. Engineering*. 7(2019), 103035, <https://doi.org/10.1016/j.jece.2019.103035>.
- [2] C. Zhang, Y. Li, D.M. Shuai, Y. Shen, D.W. Wang, Progress and challenges in photocatalytic disinfection of waterborne viruses: a review to fill current knowledge gaps. *Chem. Eng. J.* 355(2019) 399–415.
- [3] S.M. Pasini, A. Val´erio, G.Yin, J.Wang,S.M. Guelli Ulson de Souza,D.Hotza,A. de Souza, An overview on nanostructured TiO₂-containing fibers for photocatalytic degradation of organic pollutants in wastewater treatment, *Journal of Water Process Engineering*.40(2021),101827, <https://doi.org/10.1016/j.jwpe.2020.101827>.
- [4] L. Mohanty, D .S. Pattnayak, R. Singhal, D. Pradhan, S. K. Dash, Enhanced photocatalytic degradation of rhodamine B and malachite green employing BiFeO₃/g-C₃N₄

nanocomposites: An efficient visible-light photocatalyst, *Inorganic Chemistry Communications*. 138(2022),109286, <https://doi.org/10.1016/j.inoche.2022.109286>.

[5] Z.Wang, M.Gao, X.Li, J.Ning, Z.Zhou, G.li, Efficient adsorption of methylene blue from aqueous solution by graphene oxide modified persimmon tannins, *Materials Science and Engineering: C*. 108(2020),110196, <https://doi.org/10.1016/j.msec.2019.110196>.

[6]A.Y.Zahrim, N.Hilal, Treatment of highly concentrated dye solution by coagulation/flocculation–sand filtration and nanofiltration, *Water Resources and Industry*. 3(2013),23-34, <https://doi.org/10.1016/j.wri.2013.06.001>.

[7] M.F.Abid, M.A.Zablouk, A.M.Abid-Almeer, Experimental study of dye removal from industrial wastewater by membrane technologies of reverse osmosis and nanofiltration, *Iranian Journal of Env.Health sci. and Eng*. 9(2012),17, <https://doi.org/10.1186/1735-2746-9-17>.

[8] A. Ghenaatgar,R. M.A.Tehrani,A. Khadir, Photocatalytic degradation and mineralization of dexamethasone using WO₃ and ZrO₂ nanoparticles: Optimization of operational parameters and kinetic studies, *Journal of Water Process Engineering*.32(2019), 100969, <https://doi.org/10.1016/j.jwpe.2019.100969>.

[9] M. Zulfiqar, S.Chowdhury, M. Samsudina, A. Ali Siyala, A. Aziz Omar, T. Ahmada, S.Sufian, Effect of organic solvents on the growth of TiO₂ nanotubes: An insight into photocatalytic degradation and adsorption studies, *Journal of Water Process Engineering*.37(2020),101491, <https://doi.org/10.1016/j.jwpe.2020.101491>.

[10] A. Akhundi,A. Badiei,G.M. Ziarani,A. Habibi-Yangjeh,M.J. Muñoz-Batista,R. Luque, Graphitic carbon nitride-based photocatalysts: Toward efficient organic transformation for value-added chemicals production, *Molecular Catalysis*.488(2020),110902, <https://doi.org/10.1016/j.mcat.2020.110902>.

[11] A. Akhundi, A. Habibi-Yangjeh,M. Abitorabi,S.R. Pourn, Review on photocatalytic conversion of carbon dioxide to value-added compounds and renewable fuels by graphitic carbon nitride-based photocatalysts, *catalysis reviews*.61(2019),595-628, <https://doi.org/10.1080/01614940.2019.1654224>.

[12] S. Asadzadeh-Khaneghah, A. Habibi-Yangjeh, g-C₃N₄/carbon dot-based nanocomposites serve as efficacious photocatalysts for environmental purification and energy generation: A review, *Journal of Cleaner Production*.276(2020),124319, <https://doi.org/10.1016/j.jclepro.2020.124319>.

[13] A. Habibi-Yangjeh,S. Asadzadeh-Khaneghah,S. Feizpoor,A. Rouhi, Review on heterogeneous photocatalytic disinfection of waterborne, airborne, and foodborne viruses: Can we win against pathogenic viruses?, *Journal of Colloid and Interface Science*.580(2020),503-514, <https://doi.org/10.1016/j.jcis.2020.07.047>.

- [14] I.Khan, K.Saeed, N.Ali, I.Khan, B.Zhang, M.Sadiq, Heterogeneous photo degradation of industrial dyes: An insight to different mechanisms and rate affecting parameters, *Journal of Env.Chem. Engineering*.8(2020),104364, <https://doi.org/10.1016/j.jece.2020.104364>.
- [15]H.Ji, X.Jing, Y.Xu, J.Yan, H.Li, Y.Li, L.Huang, Q.Zhang, H.Xu, H.Li, Magnetic g-C₃N₄/NiFe₂O₄ hybrids with enhanced photocatalytic activity, *RSC.Adv.* 5(2015),57960-57967, <https://doi.org/10.1039/C5RA07148H>.
- [16]S. Huang, Y. Xu, M. Xie, H. Xu, M. He, J. Xia, L. Huang, H. Li, Synthesis of magnetic CoFe₂O₄/g-C₃N₄ composite and its enhancement of photocatalytic ability under visible-light, *Colloids Surfaces A Physicochem. Eng. Asp.* 478 (2015) 71–80, <https://doi.org/10.1016/j.colsurfa.2015.03.035>.
- [17] B. Janani, A. Syed, A.M. Thomas, S. Al-Rashed, L. Raju, S. Khan, Designing spinel NiCr₂O₄ loaded Bi₂O₃ semiconductor hybrid for mitigating the charge recombination and tuned band gap for enhanced white light photocatalysis and antibacterial applications, *Journal of Alloys and Compounds.* 865 (2021), 158735, <https://doi.org/10.1016/j.jallcom.2021.158735>.
- [18] B. Janani, S. Swetha, A. Syed, A.M. Elgorban, Nouf S.S. Zaghoul, Ajith M. Thomas,L.Raju, S. Khan, Spinel FeV₂O₄ coupling on nanocube-like Bi₂O₃ for high performance white light photocatalysis and antibacterial applications, *Journal of Alloys and Compounds.* 887 (2021) 161432, <https://doi.org/10.1016/j.jallcom.2021.161432>.
- [19] A.F. Shojaei, A.R. Tabari, M.H. Loghmani, Normal spinel CoCr₂O₄ and CoCr₂O₄/TiO₂ nanocomposite as novel photocatalysts,for degradation of dyes, *Micro & Nano Letters.* 8(2013), 426–431, doi: 10.1049/mnl.2013.0114.
- [20] M. Ghiyasiyan-Arani, M. Salavati-Niasari, S. Naseh, Enhanced photodegradation of dye in waste water using iron vanadate nanocomposite; ultrasound-assisted preparation and characterization,*Ultrasonics Sonochemistry.*39(2017),494-503, <https://doi.org/10.1016/j.ultsonch.2017.05.025>.
- [21] V.N. Sonkusare, R.G. Chaudhary, G.S. Bhusari, A. Mondal,A.K. Potbhare, R.K. Mishra, H.D. Juneja,A. Abdala, Mesoporous Octahedron-Shaped Tricobalt Tetroxide Nanoparticles for Photocatalytic Degradation of Toxic Dyes, *ACS Omega.* 5(2020), 7823-7835, DOI: 10.1021/acsomega.9b03998.
- [22] V.S.Kirankumar, S.Sumathi, A review on photodegradation of organic pollutants using spinel oxide,*Materials today chemistry.* 18(2020), 100355, <https://doi.org/10.1016/j.mtchem.2020.100355>.
- [23] J. Mu, L. Zhang, M. Zhao, Y. Wang, Co₃O₄ nanoparticles as an efficient catalase mimic: Properties, mechanism and its electrocatalytic sensing application for hydrogen peroxide,*J. Mol. Catal. A: Chem.* 378 (2013), 30–37, <https://doi.org/10.1016/j.molcata.2013.05.016>.

- [24] J. Jiu, Y. Ge, X. Li, L. Nie, Preparation of Co_3O_4 nano-particles by a polymer combustion route, *Mater. Lett.* 54 (2002), 260–263, [https://doi.org/10.1016/S0167-577X\(01\)00573-0](https://doi.org/10.1016/S0167-577X(01)00573-0).
- [25] S. Farhadi, K. Pourzare, S. Bazgir, Co_2O_3 nanoplates: Synthesis, characterization and study of optical and magnetic properties, *J. Alloys Compd.* 587 (2014), 632–637, <http://dx.doi.org/10.1016/j.jallcom.2013.10.259>.
- [26] O. M. Bankole, S. E. Olaseni, M. A. Adeyemo, A. S. Ogunlaja, Microwave-Assisted Synthesis of Cobalt Oxide/Reduced Graphene Oxide (Co_3O_4 -rGo) Composite and its Sulfite Enhanced Photocatalytic Degradation of Organic Dyes, *J. Phys. Chem.* 234(2020), 1681-1708, <https://doi.org/10.1515/zpch-2019-1524>.
- [27] N. N. Binitha, P. V. Suraja, Z. Yaakob, M. R. Resmi, P. P. Siliya, Simple synthesis of Co_3O_4 nanoflakes using a low temperature sol-gel method suitable for photodegradation of dyes, *J. Sol-Gel Sc. Technol.* 53 (2010), 466–469, <https://doi.org/10.1007/s10971-009-2098-8>.
- [28] U. Kamran, H.N. Bhatti, M. Iqbal, A. Nazir, Green synthesis of metal nanoparticles and their applications in different fields: a review, *Zeitschrift Fur Phys. Chemie.* 233 (2019), 1325–1349, <https://doi.org/10.1515/zpch-2018-1238>.
- [29] S.L. Gaikwad, A.P. Angre, V.A. Naik, J.G. Pargaonkar, P.A. Patil, K.V. Chandekar, A.U. Chavan, P.S. Gaikar, Binderless synthesis of nanoknotnet-like cobalt oxide for supercapacitor application, *Mater. Today Proc.*(2020), <https://doi.org/10.1016/j.matpr.2020.04.081>.
- [30] K. Kalpanadevi, C. R. Sinduja, R. Manimekalai, Characterization of nanostructured Co_3O_4 synthesized by the thermal decomposition of an inorganic precursor, *Aust. J. Chem.* 67 (2014), 1671–1674, <http://dx.doi.org/10.1071/CH13567>.
- [31] M. Mukhtar, L. Munisa, R. Saleh, Co-Precipitation Synthesis and Characterization of Nanocrystalline Zinc Oxide Particles Doped with Cu^{2+} Ions, *Materials Sciences and Applications.* 3(2012), 543-551, <http://dx.doi.org/10.4236/msa.2012.38077>.
- [32] K. Esquivel, Ma. G. García, F.J. Rodríguez, L.A. Ortiz-Frade, L.A. Godínez, Study of the photo-electrochemical activity of cobalt- and nickel-doped TiO_2 photo-anodes for the treatment of a dye-contaminated aqueous solution, *J Appl Electrochem.* 43(2013), 433–440, <https://doi.org/10.1007/s10800-013-0528-3>.
- [33] S. Faniband, Vidyasagar, V. Zemenz-perez, M. Nayaka, A. H. Shridhar, Mechanistic insight into the photocatalytic degradation of organic pollutant and electrochemical behavior of modified MWCNTs/Cu- Co_3O_4 Nano composite, *Rec.chem and eng.*(2022), <http://dx.doi.org/10.1039/D2RE00117A>.
- [34] W. Zhang, W. Shi, H. Sun, Y. Shi, H. Luo, S. Jing, Y. Fan, F. Guob, C. Luc, Fabrication of ternary $\text{CoO/g-C}_3\text{N}_4/\text{Co}_3\text{O}_4$ nanocomposite with p-n-p type heterojunction for boosted

visible-light photocatalytic performance, *J Chem Technol Biotechnol.*(2021), DOI 10.1002/jctb.6703.

[35] E. Salah Hassan, K.Yasseen Qader, E. Hassn Hadi, S.Salman Chiad, N. Fadhil Habubi , K. Haneen Abass, Sensitivity of Nanostructured Mn-Doped Cobalt Oxide Films for Gas Sensor Application, *Nano Biomed. Eng.*12(2020), 205-213, doi: 10.5101/nbe.v12i3.p205-213.

[36] M. Mayakannan, S.Gopinath,S.Vetrivel,N.Y.Maharani, Structural, morphological, optical properties of Zr- doped Co_3O_4 nanoparticles, *Particulate Science and Technology.*40(2022),664-672, <https://doi.org/10.1080/02726351.2021.1992057>.

[37] S.P. Keerthana, R. Yuvakkumar, P. Senthil Kumar, G. Ravi, Dai-Viet N. Vo, D. Velauthapillai, Influence of tin (Sn) doping on Co_3O_4 for enhanced photocatalytic dyedegradation,*Chemosphere.*277(2021),130325,*Chemosphere.*2021.130325. <https://doi.org/10.1016/j.>

[38] X. Si, G. Chen, Z. Chen, J. Huang, S. Chen, Highly catalytic $\text{Ag}/\text{Co}_3\text{O}_4$ nanocatalysts fabricated for RhB dye degradation through a simple silver-mirror reaction under visible light, *Nano Brief Reports and Reviews.*9(2014),1450090, <http://dx.doi.org/10.1142/S1793292014500908>.

[39] M. Yarahmadi, H. Maleki-Ghaleh, M.E. Mehr, Z. Dargahi, M.H. Siadati., Synthesis and characterization of Sr-doped ZnO nanoparticles for photocatalytic applications. Synthesis and characterization of Sr-doped ZnO nanoparticles for photocatalytic applications, *Catalyst*,853(2021)157000. <https://doi.org/10.1016/j.jallcom.2020.157000>

[40] D. Pradhan, P. K. Panda, A. Mishra, E. Falletta, S. K. Dash, Efficient photo-degradation of cationic dyes by Co_3O_4 and Sr- Co_3O_4 spinel nanocomposites under solar light irradiation, *Env. Qual. Mgmt, Article in press*, <https://onlinelibrary.wiley.com/doi/full/10.1002/tqem.21916>

[41] D. Prabakaran, K. Sadaiyandi, M. Mahendran, S. Sagadevan,. Precipitation method and characterization of cobalt oxide nanoparticles. *Appl. Phys. A*,123(2017) 264. DOI 10.1007/s00339-017-0786-8

[42] R. Reena, A. Aslinjensipriya, M. Jose, S. Das, Investigation on structural, optical and electrical nature of pure and Cr-incorporated cobalt oxide nanoparticles prepared via coprecipitation method for photocatalytic activity of methylene blue dye. . *J Mater Sci: Mater Electron* 31(2020)22057-22074. <https://doi.org/10.1007/s10854-020-04708-6>

[43] M. Aadil, S. Zulfiqar, M. Farooq Warsi, P. O. Agboola, I. Shakir, M.Shahid, N. F. Al-Khalli, Mesoporous and Macroporous Ag-doped Co_3O_4 Nanosheets and Their Superior Photo-Catalytic properties Under Solar Light Irradiation, *Ceramics International.*47(2021), 9806-9817, <https://doi.org/10.1016/j.ceramint.2020.12.121>.

- [44] P. Bansala, N. Bhullarb, D. Sud, Studies on photodegradation of malachite green using TiO₂/ZnO photocatalyst, *Desalination and Water Treatment*. 12 (2009), 108–113, doi: 10.5004/dwt.2009.943.
- [45] R. Sylvia Reena, A. Aslinjensipriya, M. Jose, S. Jerome Das, Investigation on structural, optical and electrical nature of pure and Cr-incorporated cobalt oxide nanoparticles prepared via co-precipitation method for photocatalytic activity of methylene blue dye, *J Mater Sci: Mater Electron*. 31(2020), 22057–22074, <https://doi.org/10.1007/s10854-020-04708-6>.
- [46] D. M. Prabakaran, K. Sadaiyandi, M. Mahendran, S. Sagadevan, Precipitation method and characterization of cobalt oxide nanoparticles, *Appl. Phys. A*. 123 (2017),264, DOI 10.1007/s00339-017-0786-8.
- [47] D. Letsholathebe, F.T. Thema, K. Mphale, H.E.A. Mohamed, K.J. Holonga, R. Ketlhwafetse, S. Chimidza, Optical and structural stability of Co₃O₄ nanoparticles for photocatalytic applications, *Materials Today: Proceedings*.36(2021), 499-503, <https://doi.org/10.1016/j.matpr.2020.05.205>.
- [48] D.M. Prabakaran, K. Sadaiyandi, M. Mahendran, S. Sagadevan, Precipitation method and characterization of cobalt oxide nanoparticles, *Appl. Phys. A* (2017), 123:264, DOI 10.1007/s00339-017-0786-8.
- [49] A.B. Vennela, D. Mangalaraj, N. Muthukumarasamy, S. Agilan, K.V. Hemalatha, Structural and Optical Properties of Co₃O₄ Nanoparticles Prepared by Sol-gel Technique for Photocatalytic Application, *Int. J. Electrochem. Sci*. 14 (2019),3535–3552, doi: 10.20964/2019.04.40.
- [50] S.K. Meher, G. Ganga Rao, Effect of Microwave on the Nanowire Morphology, Optical, Magnetic, and Pseudocapacitance Behavior of Co₃O₄, *J. Phys. Chem. C*. 115(2011), 25543–25556, <https://doi.org/10.1021/jp209165v>.
- [51] A. S. Adekunle, J. A.O. Oyekunle, L. M. Durosinmi, O. S. Oluwafemi, D.S. Olayanju, A. S. Akinola, O.R. Obisesan, O. F. Akinyele, T. A. Ajayeoba, Potential of cobalt and cobalt oxide nanoparticles as nanocatalyst towards dyes degradation in wastewater, *Nano-Structures & Nano-Objects*.21(2020),100405,<https://doi.org/10.1016/j.nanoso.2019.100405>.
- [52] A.B. Vennela, D. Mangalaraj, N. Muthukumarasamy, S. Agilan, K.V. Hemalatha, Structural and Optical Properties of Co₃O₄ Nanoparticles Prepared by Sol-gel Technique for Photocatalytic Application, *Int. J. Electrochem. Sci*. 14 (2019),3535–3552, doi: 10.20964/2019.04.40.
- [53] D. Komaraiah, E. Radhaa, J. James, N. Kalarikkal, J. Sivakumara, M.V.R. Reddy, R. Sayanna Effect of particle size and dopant concentration on the Raman and the photoluminescence spectra of TiO₂:Eu³⁺ Nano phosphor thin films, *Journal of Luminescence*.211(2019),320-333, <https://doi.org/10.1016/j.jlumin.2019.03.050>

[54] H. Zhang, S. Pokhrel, Z. Ji, H. Meng, X. Wang, S. Lin, C. Hyun Chang, L. Li, R. Li, B. Sun, M. Wang, Y. Liao, R. Liu, T. Xia, L. Mädler, A. E. Nel, PdO Doping Tunes Band-Gap Energy Levels as Well as Oxidative Stress Responses to a Co_3O_4 -Type Semiconductor in Cells and the Lung, *Am. Chem. Soc.* 136(2014), 6406-6420, <https://doi.org/10.1021/ja501699e>.

[55] S.K. Meher, G. Ganga Rao, Effect of Microwave on the Nanowire Morphology, Optical, Magnetic, and Pseudocapacitance Behavior of Co_3O_4 , *J. Phys. Chem. C.* 115(2011), 25543–25556, <https://doi.org/10.1021/jp209165v>.

[56] B. Ali Al Jahdaly, A. Abu-Rayyan, M.M. Taher, K. Shoueir, Phytosynthesis of Co_3O_4 Nanoparticles as the High Energy Storage Material of an Activated Carbon/ Co_3O_4 Symmetric Supercapacitor Device with Excellent Cyclic Stability Based on a Na_2SO_4 Aqueous Electrolyte, *ACS Omega.* 7(2022), 23673-23684, <https://doi.org/10.1021/acsomega.2c02305>.

[57] S. Sudhakar, D. N. Joshi, S. Gouse Peera, A. K. Sahu, C. M. Eggleston, R. Arun Prasath, Hydrothermal-microwave synthesis of cobalt oxide incorporated nitrogen-doped graphene composite as an efficient catalyst for oxygen reduction reaction in alkaline medium, *Journal of Materials Science: Materials in Electronics.* 29(2018), 6750-6762, <https://doi.org/10.1007/s10854-018-8661-8>.

[58] A. S. Adekunle, J. A.O. Oyekunle, L. M. Durosinmi, O. S. Oluwafemi, D.S. Olayanju, A. S. Akinola, O.R. Obisesan, O. F. Akinyele, T. A. Ajayeoba, Potential of cobalt and cobalt oxide nanoparticles as nanocatalyst towards dyes degradation in wastewater, *Nano-Structures&Nano-Objects.* 21(2020), 100405, <https://doi.org/10.1016/j.nanoso.2019.100405>.

[59] R. Bhargava, S. Khana, N. Ahmad, M. M. Nizam Ansari, Investigation of structural, optical and electrical properties of Co_3O_4 nanoparticles, *AIP conference proceedings.* 1953(2018), 030034, <https://doi.org/10.1063/1.5032369>.

[60] P.B. Koli, K.H. Kapadnis, U. G. Deshpande, M.R. Patil, Fabrication and characterization of pure and modified Co_3O_4 nanocatalyst and their application for photocatalytic degradation of eosine blue dye: a comparative study, *Journal of Nanostructure in Chemistry.* 8(2018), 453-463, <https://doi.org/10.1007/s40097-018-0287-0>.

[61] A.M. Tonelli, J. Venturini, S. Arcaro, J. G. Henn, D.J. Moura, A. da Cas Viegas, C. P. Bergmann, Novel core-shell nanocomposites based on TiO_2 -covered magnetic Co_3O_4 for biomedical applications, *Journal of Biomedical Materials Research.* 108(2019), 1879-1887, <https://doi.org/10.1002/jbm.b.34529>

[62] A.K. Sharma, B.K. Lee, Adsorptive/photo-catalytic process for naphthalene removal from aqueous media using in-situ nickel doped titanium nanocomposite, *Journal of Environmental Management.* 155(2015), 114-122, <http://dx.doi.org/10.1016/j.jenvman.2015.03.008>.

[63] C. R. Dhas, R. Venkatesh, K. Jothivenkatachalam, A. Nithya, B. Suji Benjamin, A. M. E. Raj, K. Jeyadheepan, C. Sanjeeviraja, Visible light driven photocatalytic degradation of

Rhodamine B and Direct Red using cobalt oxide nanoparticles, *Ceramics International*.41(2015), 9301-9313, <https://doi.org/10.1016/j.ceramint.2015.03.238>.

[64]R. Monsef, M. Ghiyasiyan-Arani, M. Salavati-Niasari, Application of Ultrasound-Aided Method for the Synthesis of NdVO₄ Nanophotocatalyst and Investigation of Eliminate Dye in Contaminant Water, *Ultrasonics Sonochemistry*. 42(2018),201-211, <https://doi.org/10.1016/j.ultsonch.2017.11.025>

[65] L.Mohanty,D.S.Pattnaik,S.K.Dash, An efficient ternary photocatalyst Ag/ZnO/g-C₃N₄ for degradation of RhB and MG under solar radiation, *Journal of the Indian Chemical Society*.98(2021),100180, <https://doi.org/10.1016/j.jics.2021.100180>

[66]T. Warang, N. Patel, R. Fernandes, N. Bazzanella, A. Miotello, Co₃O₄ nanoparticles assembled coatings synthesized by different techniques for photo-degradation of methylene blue dye, *Applied Catalysis B: Environmental*.132(2013),204-211, <https://doi.org/10.1016/j.apcatb.2012.11.040>.

[67]S. Farhadi, M. Javanmard, G. Nadr, Characterization of Cobalt Oxide Nanoparticles Prepared by the Thermal Decomposition of [Co(NH₃)₅(H₂O)](NO₃)₃ Complex and Study of Their Photocatalytic Activity, *Acta Chim. Slov*.63(2016),335-343, DOI: 10.17344/acsi.2016.2305.

[68]R. S. Reena, A. Aslinjensipriya, S. G. Infantiya, J. Daniel John Britto, M. Jose, S. J. Das, Visible- light active zinc doped cobalt oxide (Zn-Co₃O₄) nanoparticles for photocatalytic and photochemical activity, *Materials Today: Proceedings*.(2022), <https://doi.org/10.1016/j.matpr.2022.05.167>.

[69]M. Gogoi, B. K. Das, Photocatalytic Degradation of Organic Dyes by Nanostructured Cobalt Oxides under UV-light, *Journal of Chemistry and Chemical Sciences*. 7(8)(2017), 565-574,

[70]N. Abbas, N. Rubab, N. Sadiq, S.Manzoor, M. Imran Khan, J. Fernandez Garcia, I. Barbosa Aragao, M.Tariq, Z. Akhtar, G. Yasmin, Aluminum-Doped Cobalt Ferrite as an Efficient Photocatalyst for the Abatement of Methylene Blue, *water*.12(2020),2285, <https://doi.org/10.3390/w12082285>.

[71]H. Javed, A. Rehman,S. Mussadiq, M. Shahid, M. Azhar Khan, I. Shakir, P. Olaleye Agboola, M.F. Aly Aboud, M. Farooq Warsi, Reduced graphene oxide-spinel ferrite nano-hybrids as magnetically separable and recyclable visible light driven photocatalyst, *Synthetic Metals*.254(2019),1-9, <https://doi.org/10.1016/j.synthmet.2019.05.013>.

[72]R. Mimouni, B. Askri, T. Larbi, M. Amlouk, A. Meftah, Photocatalytic degradation and photo-generated hydrophilicity of Methylene Blue over ZnO/ZnCr₂O₄ nanocomposite under stimulated UV light irradiation, *Inorg. Chem. Comm*.115(2020),107889, <https://doi.org/10.1016/j.inoche.2020.107889>.

[73]S. Alkaykh, A. Mbarek, E. Ali-Shattle, Photocatalytic degradation of methylene blue dye in aqueous solution by MnTiO_3 nanoparticles under sunlight irradiation, *Heliyon*.6(2020),e03663, <https://doi.org/10.1016/j.heliyon.2020.e03663>.

[74]M. Arunkumar, A. S. Nesaraj, Facile chemical fabrication of Ni doped CoAl_2O_4 nano-spinel photocatalysts: Physico-chemical properties and photodegradation of toxic malachite green dye under visible light, *Inter. J. Env. Anal. Chem.*(2020), <https://doi.org/10.1080/03067319.2020.1867722>.

[75] J. Tao, M. Zhang, X. Gao, H. Zhao, Z. Ren, D. Li, J. Li, R. Zhang, Y. Liu **, Y. Zhai, Photocatalyst Co_3O_4 /red phosphorus for efficient degradation of malachite green under visible light irradiation, *Materials Chemistry and Physics*.240(2020),122185, <https://doi.org/10.1016/j.matchemphys.2019.122185>.

[76] M. A. Salam, M. R. Abukhadra, A. Adlii, Insight into the Adsorption and Photocatalytic Behaviors of an Organo-bentonite/ Co_3O_4 Green Nanocomposite for Malachite Green Synthetic Dye and Cr(VI) Metal Ions: Application and Mechanisms, *ACS Omega*.5(2020),2766-2778, <https://doi.org/10.1021/acsomega.9b03411>.

[77]S. Akshatha, S. Sreenivasa, L. Parashuram, V. Udaya kumar, F.A. Alharthi, T. M. Chakrapani Rao, S. kumar, Microwave assisted green synthesis of p-type Co_3O_4 @Mesoporous carbon spheres for simultaneous degradation of dyes and photocatalytic hydrogen evolution reaction, *Materials Science in Semiconductor Processing*.121(2021),105432, <https://doi.org/10.1016/j.mssp.2020.105432>.

[78]N. Arsalani, S. Bazazi, M. Abuali, S. Jodeyri, A new method for preparing ZnO/CNT nanocomposites with enhanced photocatalytic degradation of malachite green under visible light, *Journal of Photochemistry & Photobiology, A: Chemistry*.389(2020),112207, <https://doi.org/10.1016/j.jphotochem.2019.112207>.

[79]M. F. Elkady, H. Shokry Hassan Photocatalytic Degradation of Malachite Green Dye from Aqueous Solution Using Environmentally Compatible Ag/ZnO Polymeric Nanofibers, *Polymers*.13(2021),2033, <https://doi.org/10.3390/polym13132033>.

[80] M. Arunkumar, A. Samson Nesaraj, Photocatalytic degradation of malachite green dye using NiAl_2O_4 and Co doped NiAl_2O_4 nano photocatalysts prepared by simple one pot wet chemical synthetic route, *Iranian Journal of Catalysis*. 10(3) (2020), 235-245,

[81] L. Mohanty, D. S. Pattanayak, D. Pradhan, S. K. Dash, Synthesis of novel p-n heterojunction g- C_3N_4 / $\text{Bi}_4\text{Ti}_3\text{O}_{12}$ photocatalyst with improved solar-light-driven photocatalytic degradation of organic dyes, *Env. Qual Mgmt*(2022),1-15, DOI: 10.1002/tqem.21907

[82]P. Vinosha, L.A. Annie, J.E. Mely, S.K. Jeronsia, S. Jerome Das, Synthesis and properties of spinel ZnFe_2O_4 nanoparticles by facile co-precipitation route, *Optik*. 134(2017), 99–108, <https://doi.org/10.1016/j.ijleo.2017.01.018>.

[83]S. Munir, A. Rasheed, S. Zulfiqar, M. Aadil, P.O. Agboola, I. Shakir, M.F. Warsi, Synthesis, characterization and photocatalytic parameters investigation of a new $\text{CuFe}_2\text{O}_4/\text{Bi}_2\text{O}_3$ nanocomposite, *Ceramics International*. 46(2020), 29182-29190, <https://doi.org/10.1016/j.ceramint.2020.08.091>.

[84]L. Mohanty, D. S. Pattanayak, S. K. Dash, R. Singhal, D. Pradhan, Enhanced photocatalytic degradation of rhodamine B and malachite green employing $\text{BiFeO}_3/\text{g-C}_3\text{N}_4$ nanocomposites: An efficient visible-light photocatalyst, *Inorganic Chemistry Communications*. 138(2022),109286, <https://doi.org/10.1016/j.inoche.2022.109286>.